***Supplementary Material* for:**

The limits of edge bead planarization and surface levelling in spin-coated liquid films

Steve Arscott

Institut d'Electronique, de Microélectronique et de Nanotechnologie (IEMN), CNRS UMR8520, The University of Lille, Cité Scientifique, 59652 Villeneuve d'Ascq, France.

E-mail: steve.arscott@univ-lille.fr

1. Derivation of Equations 2a and 2b in the article

The fluid flow Q ($m^2\ s^{-1}$) in the film is given by the following expression:

$$Q = \frac{h^3}{3\eta} f$$

Where h is the thickness of the liquid film (equation 1 in the manuscript), f ($N\ m^{-3}$) is the volume force, and η is the dynamic viscosity (Pa s) of the liquid. The force f in the case of either surface tension-driven (f_γ) or gravity-driven (f_g) flow is given by the following expressions:

$$f_\gamma = \gamma q^3 \delta \sin(qx)$$

$$f_g = \rho g q \delta \sin(qx)$$

As an aside, in the case of the gravity-driven situation, the product ρg is known historically as the *specific weight*, by comparing the two equations we can see that for the surface tension-driven situation, the equivalent of this specific weight is the product γq^2 or $4\pi^2\gamma/\lambda^2$. Combining, expanding, and

approximating the above equations by taking only the first order terms of δ (the full expansions can be found below in section 2), gives the following expressions for the one-dimensional fluid flow Q in terms of the physical properties of the liquid and the critical dimensions of the system—again, for both surface tension-driven and gravity-driven flow we have:

$$Q_\gamma = \frac{\gamma \delta h_\infty^3 q^3 \sin(qx)}{3\eta}$$

$$Q_g = \frac{\rho g \delta h_\infty^3 q \sin(qx)}{3\eta}$$

From fluid dynamics theory we know that:

$$\frac{\partial Q}{\partial x} = -\frac{\partial h}{\partial t}$$

By differentiating, expanding, and approximating by using only the first order terms of δ, the differentials of the flow dQ/dx can be approximated by the following expressions, again in the case of surface tension-driven and gravity-driven flow:

$$\frac{\partial Q_\gamma}{\partial x} = \frac{\gamma \delta h_\infty^3 q^4 \cos(qx)}{3\eta}$$

$$\frac{\partial Q_g}{\partial x} = \frac{\rho g \delta h_\infty^3 q^2 \cos(qx)}{3\eta}$$

By using the above equations and knowing that $\partial h/\partial t = \partial \delta/\partial t$, and introducing the notion of a time-dependent surface tension $\gamma(t)$, density $\rho(t)$, and viscosity $\eta(t)$ we can now write down:

$$\frac{\partial \delta}{\partial t} = -\frac{\gamma(t) \delta h_\infty^3 q^4 \cos(qx)}{3\eta(t)}$$

$$\frac{\partial \delta}{\partial t} = -\frac{\rho(t) g \delta h_\infty^3 q^2 \cos(qx)}{3\eta(t)}$$

As δ_0 is at the maximum of the perturbation, we have $\cos(qx) = 1$, therefore:

$$\frac{\partial \delta}{\partial t} = -\frac{\gamma(t)\delta h_\infty^3 q^4}{3\eta(t)}$$

$$\frac{\partial \delta}{\partial t} = -\frac{\rho(t) g \delta h_\infty^3 q^2}{3\eta(t)}$$

Note that δ is the dependent variable, t is the independent variable—$\gamma(t)$, $\eta(t)$, and $\rho(t)$ can be written down as functions of time. Thus, by separating variables we have:

$$\int \frac{1}{\delta} d\delta = -K_\gamma \int \frac{\gamma(t)}{\eta(t)} dt$$

$$\int \frac{1}{\delta} d\delta = -K_g \int \frac{\rho(t)}{\eta(t)} dt$$

Where

$$K_\gamma = \frac{h_\infty^3 q^4}{3}$$

$$K_g = \frac{g h_\infty^3 q^2}{3}$$

Integrating the left hand side gives us Equations 2a and 2b in the article:

$$\ln \delta + C_\gamma^1 = -K_\gamma \int \frac{\gamma(t)}{\eta(t)} dt$$

$$\ln \delta + C_g^1 = -K_g \int \frac{\rho(t)}{\eta(t)} dt$$

2. Full expansions of the reflows and differentials of the reflows

The fully-expanded expressions of the reflows Q and differentials of the reflows $\partial Q/\partial x$, with respect to lateral distance x, are given below.

2.1 Surface tension-driven flow

$$Q = \frac{\delta^4 \gamma q^3 \sin^4 qx}{3\eta} + \frac{\delta^3 \gamma h_\infty q^3 \sin^3 qx}{\eta} + \frac{\delta^2 \gamma h_\infty^2 q^3 \sin^2 qx}{\eta} + \frac{\delta \gamma h_\infty^3 q^3 \sin qx}{3\eta}$$

$$\frac{dQ}{dx} = \frac{4\delta^4 \gamma q^4 \sin^3 qx \cos qx}{3\eta} + \frac{3\delta^3 \gamma h q^4 \sin^2 qx \cos qx}{\eta} + \frac{2\delta^2 \gamma h^2 q^4 \sin qx \cos qx}{\eta} + \frac{\delta \gamma h^3 q^4 \cos qx}{3\eta}$$

2.2 Gravity-driven flow

$$Q = \frac{\delta^4 \rho g q \sin^4 qx}{3\eta} + \frac{\delta^3 \rho g h_\infty q^3 \sin^3 qx}{\eta} + \frac{\delta^2 \rho g h_\infty^2 q \sin^2 qx}{\eta} + \frac{\delta \rho g h_\infty^3 q \sin qx}{3\eta}$$

$$\frac{dQ}{dx} = \frac{4\delta^4 \rho g q^2 \sin^3 qx \cos qx}{3\eta} + \frac{3\delta^3 \rho g h_\infty q^2 \sin^2 qx \cos qx}{\eta} + \frac{2\delta^2 \rho g h_\infty^2 q^2 \sin qx \cos qx}{\eta} + \frac{\delta \rho g h_\infty^3 q^2 \cos qx}{3\eta}$$

3. The variation of the viscosity and the density of drying SU-8 with time

The manufacturers of SU-8 (MicroChem, USA) give data concerning how the density of the SU-8 photoresist (ρ_{SU-8}) i.e. solids content (dry matter) plus solvents, and the kinematic viscosity μ_{SU-8} vary with solids content S (%). This data has been published [1]. In this Supplementary Section, I will describe a practical method which can be used to obtain the variation of the dynamic viscosity η_{SU-8} and the density ρ_{SU-8} of a thick film of SU-8 photoresist during drying.

In its liquid form, SU-8 photoresist is composed of solids (epoxy resin, bis-triarylsulfonium and sulfonium hexafluoroantimonate salts) and a solvent (cyclopentanone $(CH_2)_4CO$). The 'solid matter content'-to-'solvent matter content' ratio determines the 'grade' of SU-8 e.g. 2002, 2005…2100. Both the viscosity and density of the photoresist are dependent on the solid matter content S of the photoresist. The density of the solid matter in the SU-8 photoresist ρ_{solid} is ~1450 kg m^{-3}. The density of the solvent (cyclopentanone) $\rho_{solvent}$ is 950 kg m^{-3}. The surface tension of SU-8 photoresist is reported to be ~45 mJ m^{-2} [2].

The experimental procedure is simple. We are going to spin coat a thick film of SU-8 photoresist onto a solid disc (wafer) of known weight. We are going to accurately measure how the weight of this *ensemble* (disc plus SU-8) varies with time. By subtracting the mass of the disc from this data we can evaluate the absolute solvent loss (and the solvent loss rate) with time. We can use this to calculate how the solids content S of SU-8 varies with time. By knowing this, we can use the published manufacture's data to plot how the density and dynamic viscosity of SU-8 photoresist vary with time. These data plots enable analytical functions $\eta_{SU-8}(t)$ and $\rho_{SU-8}(t)$ to be fitted. These analytical functions are then used to compute the reflow fluid dynamics during planarization.

Before proceeding, let us denote the following quantities which are measured and used in the subsequent analysis: m_{SU-8} is the total mass of the SU-8 photoresist (solids + solvents) in the spin coated thick film, m_{solid} to be the mass of the solid content of the SU-8 film—this is constant, $m_{solvent}$ is the

mass of the solvent in the SU-8 film—this reduces with time due to evaporation, and m_{disc} is the mass of the silica disc prior to the spin coating of the SU-8.

In terms of density, according to the manufacture's data the density of the SU-8 photoresist is plotted in the figure as a function of solids content.

In terms of viscosity, the manufactures of SU-8 provide data on how the kinematic viscosity (cSt) of SU-8 photoresist varies with solids content. In order to convert the kinematic viscosity ν (cSt) to dynamic viscosity η (Pa s) one uses the following formula: $\eta = \rho\nu \times 10^{-6}$, where ρ is the density of the liquid photoresist at a given solids content. The dynamic viscosity of SU-8 photoresist is plotted as a function of solids content in the figure below.

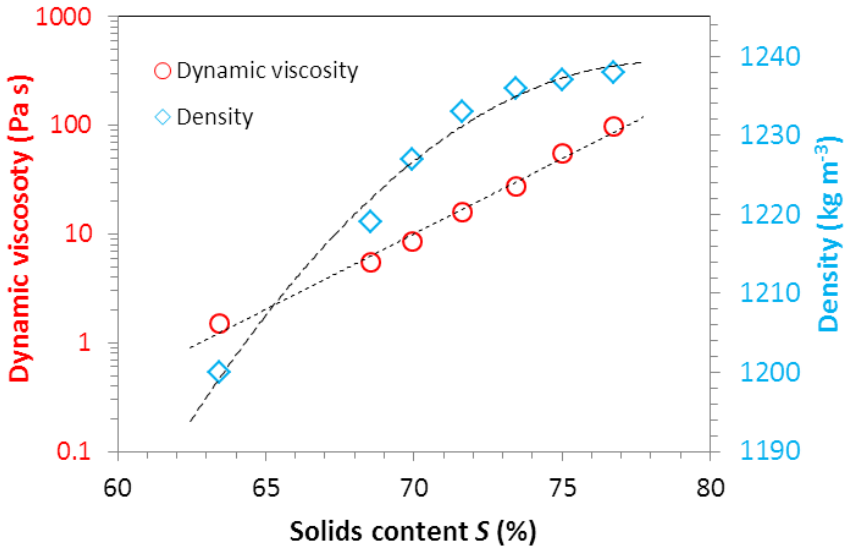

Supplementary Figure S1. The variation of the dynamic viscosity (Pa s) and the density of SU-8 photoresist as a function of solids content S (%). The data is taken from manufacture's data sheet. The dashed black lines are fits using analytical formulae (see text).

The density (kg m^{-3}) of SU-8 can be approximated by the following second order polynomial fit which has a coefficient of determination (R^2) equal to 0.99:

$$\rho(S) = -0.18S^2 + 28.27S + 132$$

The dynamic viscosity (Pa s) of SU-8 can be approximated by the following exponential fit which also has a coefficient of determination (R^2) equal to 0.99:

$$\eta(S) = 1.98 \times 10^{-9} e^{0.32S}$$

In order to find how the density and dynamic viscosity of SU-8 photoresist changes with time we need to find how the solids content S evolves with time. This will evidently depend on evaporation of the solvent from the SU-8 photoresist which depends on the evaporation conditions. Here we perform this in the context of reflow planarization of a thick film so the experiments are performed on a spin-coated thick film of SU-8 at room temperature.

The following paragraph describes the fabrication of the samples. All fabrication and experiments were conducted in a class ISO 5/7 cleanroom. SU-8 2035 photoresist (MicroChem, USA) was spin-coated using a commercial spin-coater onto 50 mm diameter, ~175 µm thick commercial silica discs (Thermo Scientific, Germany) at a spin speed of 1000 rpm in order to achieve a nominal thickness of 150 µm. Two sets of samples were prepared. The first set intended for planarization—the second set intended for immediate photoresist 'pre-bake' on a hot plate at 95°C.

The follow paragraph describes the measurements. In order to estimate how the viscosity and density changes with time (due to solvent evaporation) one can accurately weigh the SU-8 as a function of time. The weighing of the samples was done using a precision micro balance XPR6UD5 (Mettler Toledo, USA). The readability and repeatability of the microbalance is 0.0005 mg and 0.0007 mg—after 1000 minutes of continuous measurement, the drift was evaluated to be 0.0375 mg in this specific experimental setup (*NB* the top cover of the microbalance was removed to allow solvents to escape). Prior to spin-coating, the mass of the silica discs (m_{disc}) was measured in each case. Immediately following the spin coating the combined mass of the SU-8 photoresist plus the silica disc was measured to enable the mass of the SU-8 photoresist to be evaluated by subtracting the mass of the disc. Following this, the mass of the

sample was measured periodically over a period of 1000 minutes (~16 hours). The figure below shows how the mass of the photoresist m_{SU-8} (mg) and the solids content *S* of the SU-8 photoresist evolve with time. The solids content of the photoresist is computed from the ratio of the solid mass of SU-8 in the photoresist—measured at time zero—which presumably remains constant. At time zero *S* = 69.95% for SU-8 2035.

$$\frac{S}{100} = \frac{m_{solid}}{m_{SU-8}}$$

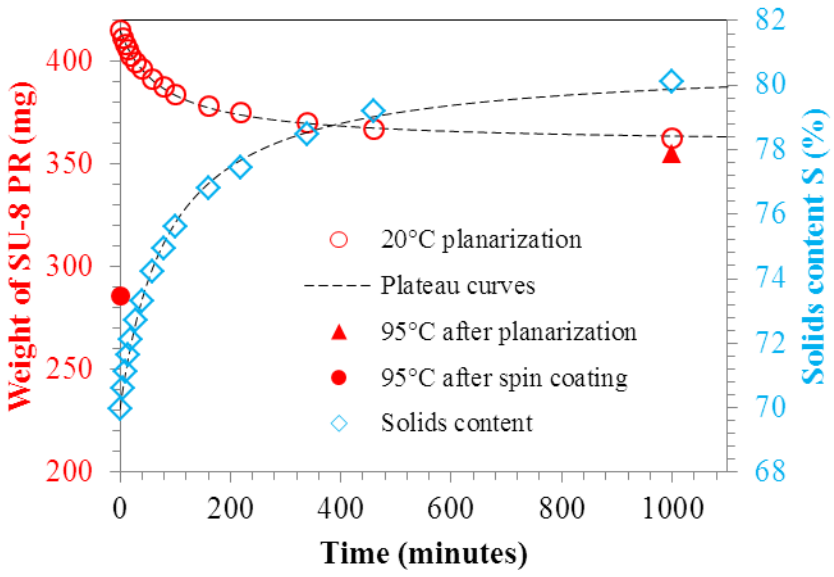

Supplementary Figure S2. The variation of the weight of the SU-8 photoresist (m_{SU-8}) and the solids content of the SU-8 photoresist (S) plotted as a function of time. The dashed lines correspond to fits (Plateau curves). The solid data points are measurements after heating the SU-8—directly after spin coating (filled red circle) and following planarization. A second silica disc sample, coated with SU-8 and heated directly after spin coating (95°C for 30 minutes), was used to generate the data point (filled red circle) at *t* = 0.

It was discovered that Plateau curves accurately fit the experimental data. In the case of the variation of the mass of the SU-8 photoresist we have:

$$m_{SU-8} = -\frac{\alpha t}{\beta + t} + \gamma$$

where α, β, and γ are constants—in the case here, they are determined to be 55.5, 75, and 415.45. The equation above relating S, m_{solid}, and m_{SU-8} can be thus used to determine the relationship between the solids contents and the time—also a Plateau curve.

The weight of the solvent content $m_{solvent}$ and the computed solvent loss rate can be plotted. The figure below shows this.

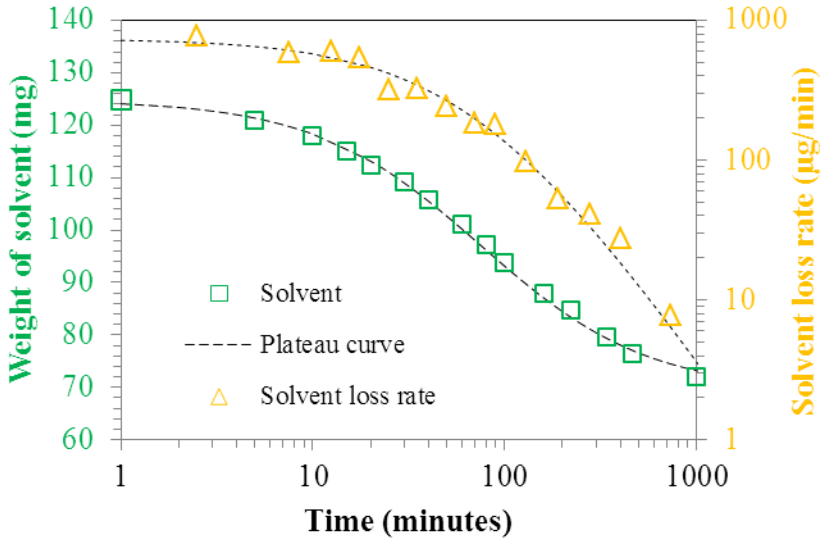

Supplementary Figure S3. The solvent content weight $m_{solvent}$ and solvent loss rate $dm_{solvent}/dt$ of SU-8 photoresist plotted as a function of time.

Evidently, the solvent content can also be fitted accurately with a Plateau curve. By differentiating this function with respect to time, we can write down the following formula describing the solvent loss rate from the SU-8 photoresist:

$$\frac{dm_{SU-8}}{dt} = \frac{dm_{solvent}}{dt} = -\frac{\alpha\beta}{(\beta + t)^2}$$

where α, β, and γ are the constants given above. This function is plotted as the short dashed curve in the figure above.

We are now in a position to plot the dynamic viscosity and the density of the SU-8 photoresist as a function of time and write down analytical expressions for these functions.

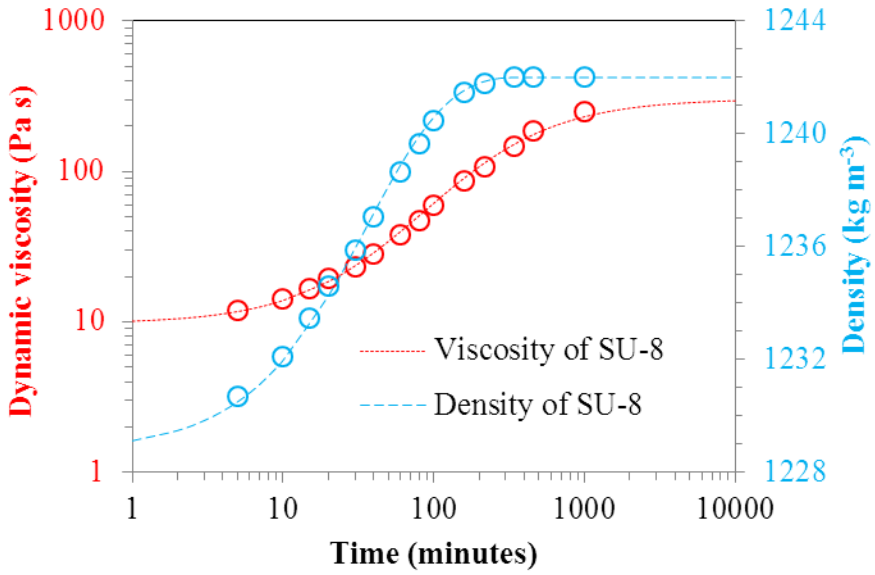

Supplementary Figure S4. The dynamic viscosity and density of SU-8 photoresist plotted as a function of time. The data points correspond to values given by the manufacturer plotted as a function of time using the method described here. The dashed lines are analytical fits (see text).

We have seen that the dynamic viscosity of SU-8 varies with the solids content according to:

$$\eta(S) = Ae^{BS}$$

where A = 1.98×10^{-9} and B = 0.319, and

$$S(t) = \frac{100 m_{solid}}{\gamma - \frac{\alpha t}{\beta + t}}$$

The time-varying viscosity and density of SU-8 photoresist can be thus approximated by the following analytical expressions:

$$\eta_{SU-8}(t) = 1.98 \times 10^{-9} e^{\frac{31.9 m_{solid}}{\gamma - \frac{\alpha t}{\beta + t}}}$$

$$\rho_{SU-8}(t) = -0.18\left(\frac{100 m_{solid}}{\gamma - \frac{\alpha t}{\beta + t}}\right)^2 + 28.27\left(\frac{100 m_{solid}}{\gamma - \frac{\alpha t}{\beta + t}}\right) + 132$$

or:

$$\rho_{SU-8}(t) = -1805\left(\frac{m_{solid}}{\gamma - \frac{\alpha t}{\beta + t}}\right)^2 + 2827\left(\frac{m_{solid}}{\gamma - \frac{\alpha t}{\beta + t}}\right) + 132$$

Parameter	Numerical value
α	55.5
β	75
γ	415.45
A	1.98×10^{-9}
B	0.319

Supplementary Table 1. List of parameters and their numerical values used for the fitting of the SU-8 data.

4. Experimental planarization of SU-8 spin coated onto silicon wafers

The following section describes how the experimental data points for the planarization of the SU-8 presented in the manuscript were obtained.

SU-8 2035 (Microchem, USA) was spin coated onto polished 2-inch diameter silicon wafers (Siltronix, France)—a commercial spin coater was used for this task. The thickness of each wafer was measured carefully using a commercial thickness gauge/comparator (Mitutoyo, Japan)—accurate to within ±1 μm. The silicon wafers were spin coated with 4 ml of SU-8 at 1000rpm, 700rpm, and 400rpm (300 rpm s^{-1} for 30s). Following spin coating, half the wafers were immediately annealed on a leveled (±0.1°) hot plate set to a temperature of 95°C. The other half of the spin-coated wafers was placed (one by one) onto a pre-cooled metal block (~4°C) having a thickness of ~1 cm in an effort to increase the viscosity of the SU-8 and initially reduce reflow. The reason for this was to be able to measure the initial height of the edge bead *directly after spin coating*. This was performed using a VHX-6000 digital microscope (Keyence, Japan) by focusing on deliberately-introduced micro-bubbles on the SU-8 surface. Once the initial edge bead height had been estimated using this method, these samples were placed on pre-leveled (±0.1°) metal blocks and left to planarized for 24 hours.

The surface profiles of all the samples were gathered using a DektakXT surface profiler (Bruker, USA) and analyzed using Vision64 software (Bruker). The SU-8 film thickness of all samples was gathered using the commercial thickness gauge/comparator.

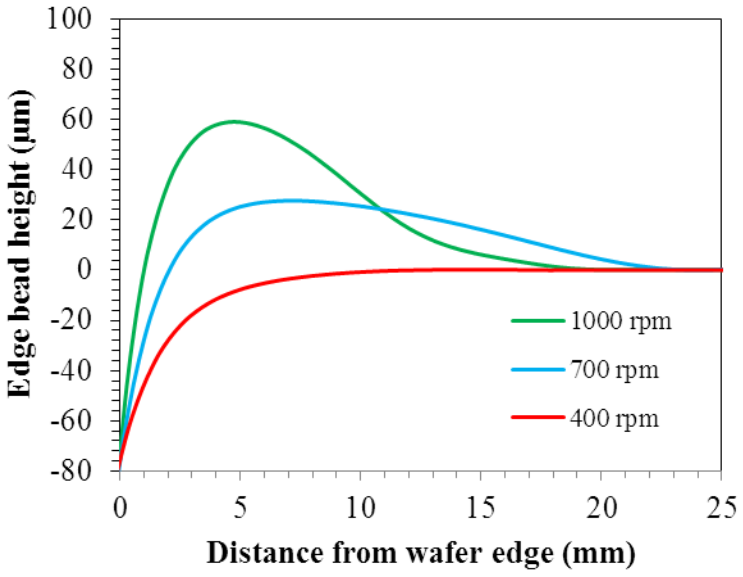

Supplementary Figure S5. Surface profiles of SU-8 samples heated to 95°C directly after spin coating.

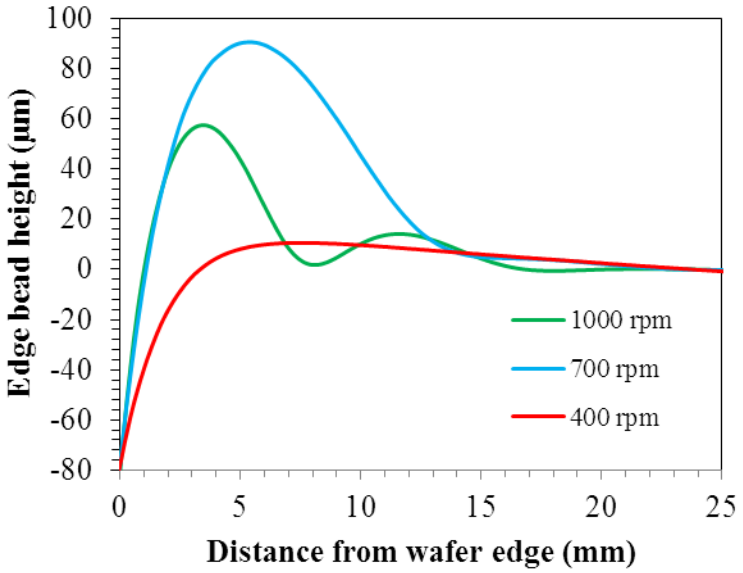

Supplementary Figure S6. Surface profiles of SU-8 samples planarized for 24 hours at 20°C.

Supplementary Figures S5 and S6 show the experimental results of the surface profiling of the spin-coated SU-8 samples.

5. The variation of the viscosity of curing polydimethylsiloxane with time

The literature provides enough data to be able to estimate how the viscosity of polydimethylsiloxane (Sylgard 184 having a 10:1 base/curing agent mixture) changes with time at various fixed curing temperatures. First, we have the 'time to curing' given by the manufacturer i.e. the time to where the viscosity achieves saturation to a *saturated* viscosity η_∞ (at a given curing temperature) when polymerization reaction stops (at a given curing temperature). Second, we have the *initial* viscosity η_0 of PDMS mixture as a function of curing temperature *before polymerization starts* [3]. Third, the literature provides some data indicating how the viscosity changes between these two values of viscosity [4].

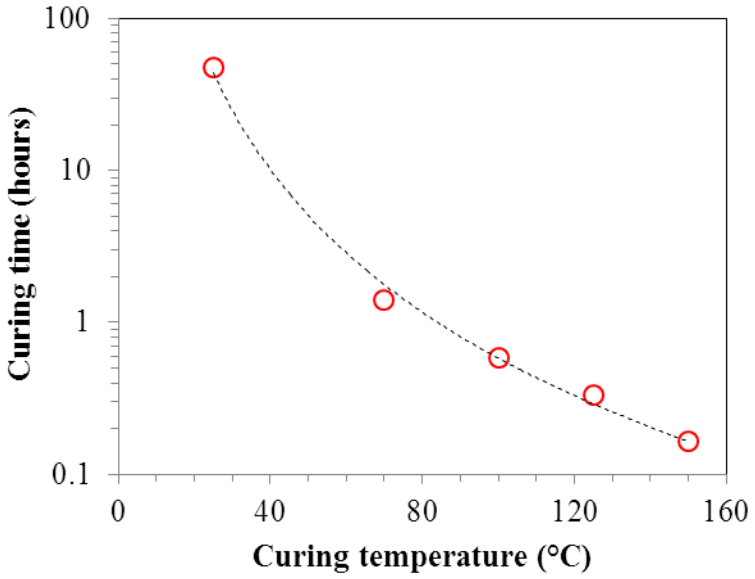

Supplementary Figure S7. Curing time t_c of polydimethylsiloxane (10:1 Sylgard 184, Dow Corning) versus temperature. This data is obtained from the manufacturer's data sheet. The dotted black line corresponds to the relationship $t_c = 1 \times 10^6 T^{-3.12}$ (with a coefficient of determination equal to 0.996).

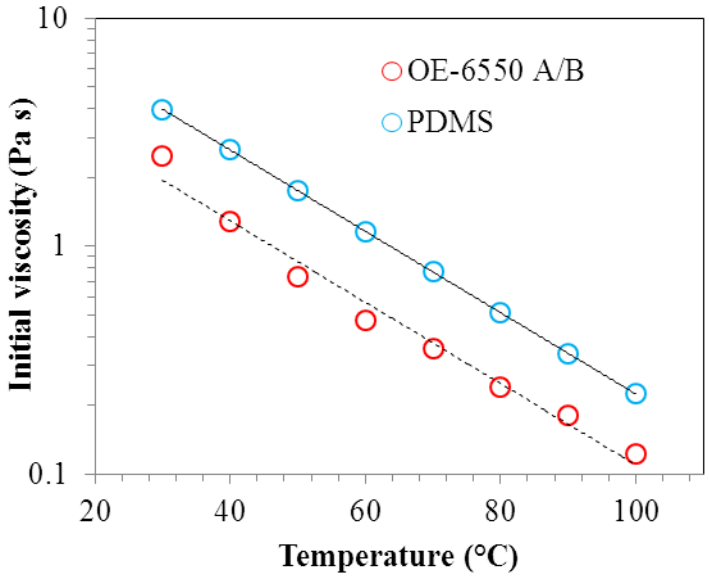

Supplementary Figure S8. Initial viscosity η_0 versus temperature for a commercial two component silicone (OE-6550 A/B) made by Dow Corning (red data points) [3]. A model for the viscosity of polydimethylsiloxane (10:1 Sylgard 184, Dow Corning) (blue circles).

The temperature T variation of the initial viscosity of the two component silicone (OE-6550 A/B) made by Dow Corning can be approximated by the following relationship:

$$\eta_0(T) = 6.68e^{-T/24.34}$$

The initial viscosity of the PDMS can be estimated by looking at data in the literature. Shu *et al* [3]. report the viscosity (in the first few minutes of curing) for a two component silicone. Based on this data, one can estimate the initial viscosity of polydimethylsiloxane versus temperature in the initial phase (<1 minute) of the curing using the following relationship:

$$\eta_0 = 13.7e^{-T/24.34}$$

This is plotted at the blue circles. The above equations agree with the work of Barlow *et al* [5] who studied the variation of viscosity of polydimethylsiloxane liquid with temperature—their data confirmed the model proposed by Williams *et al* [6].

Data in the literature describing how the viscosity of PDMS changes with time during curing can be plotted—this is shown in the figure.

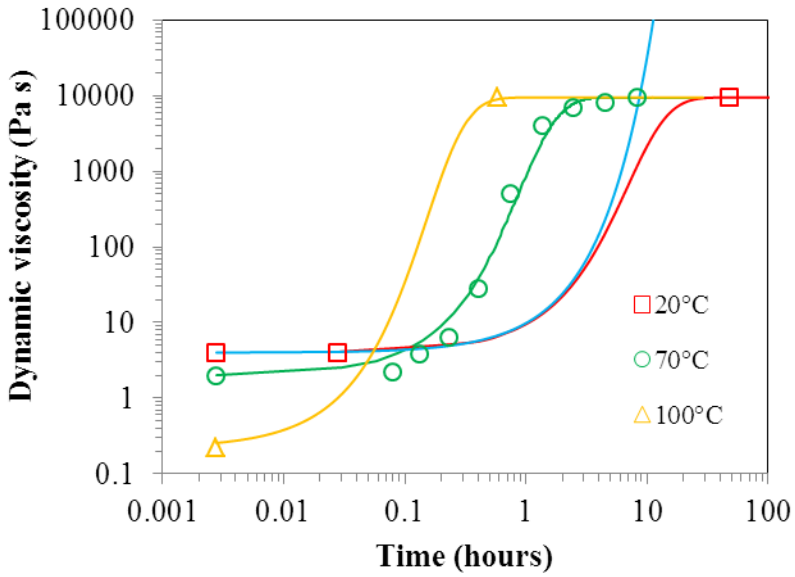

Supplementary Figure S9. The variation of the viscosity of PDMS with time during curing. The figure shows data points found in the literature and analytical models developed in the current work. The exponential rise model is shown by the light blue curve. The exponential rise and saturation are given by the yellow, green, and red curves.

We are now in a position to fit an analytical function to model how the viscosity of curing polydimethylsiloxane changes with time. First we can consider an exponential rise of the viscosity (see blue curve in the figure).

$$\eta_{PDMS}(t) = \eta_0 e^{t/\tau_\eta}$$

Second, we can consider an exponential rise followed by saturation (see red curve in the figure).

$$\eta_{PDMS}(t) = \frac{\eta_0^2}{\eta_\infty} e^{\left(\frac{2\ln(\eta_\infty/\eta_0)}{1+e^{-t/\tau_\eta}}\right)}$$

The fluid properties of liquid PDMS

The Supplementary Table below gives the fluid properties of freshly prepared, pre-cured PDMS mixture. The surface tension was measured for 'polymethylsiloxane' base [7]. The Density and dynamic viscosity were measured for mixed 10:1 PDMS (mixed per-cured Sylgard™ 184 10:1 in liquid form) [8–10].

Property	**Symbol**	**Value**	**Units**	**Ref.**
Surface tension	γ	19.9	mJ m^{-2}	Fox and Zisman [7]
Density	ρ	970	Kg m^{-3}	Bates [8], Mark [9]
Dynamic viscosity	η	3.74-4.14	Pa s	Rolland *et al* [10], Schneider *et al* [11]

Supplementary Table 2. Summary of properties of freshly prepared, pre-cured liquid polydimethylsiloxane (PDMS) mixture at room temperature.

6. Experimental planarization of PDMS spin coated onto silicon wafers

The following section describes how the experimental data points for the planarization of the PDMS presented in the manuscript were obtained.

PDMS (Dow Corning, USA) was spin coated onto polished 3-inch diameter silicon wafers (Siltronix, France). A commercial spin coater Delta 10 BM (Suss MicroTec Lithography GmbH, Germany) was used to coat the silicon wafers with the PDMS mixture. The base/curing agent weight ratio was 10:1. The thickness of each silicon wafer was measured carefully using a commercial thickness gauge/comparator (Mitutoyo, Japan)—accurate to within ±1 μm. The silicon wafers were spin coated with 8 ml of PDMS mixture at 500 rpm and 350 rpm (350 rpm s^{-1} for 30s). Following spin coating of the PDMS, half the wafers were immediately annealed in a leveled (±0.1°) box furnace set to a temperature of 100°C. The other half of the spin-coated wafers was placed (one by one) onto a pre-cooled metal block (~4°C) having a thickness of ~1cm in an effort to increase the viscosity of the PDMS and initially reduce reflow. The reason for this was to be able to measure the initial height of the edge bead *directly after spin coating*. This was performed using a VHX-6000 digital microscope (Keyence, Japan) by focusing on deliberately-introduced micro-bubbles on the PDMS surface. Once the initial edge bead height had been estimated using this method, these samples were placed on pre-leveled (±0.1°) metal blocks and left to planarized for 24 h.

The surface profiles of all the samples were gathered using a DektakXT surface profiler (Bruker, USA) and analyzed using Vision64 software (Bruker). The PDMS film thickness of all samples was gathered using the commercial thickness gauge/comparator.

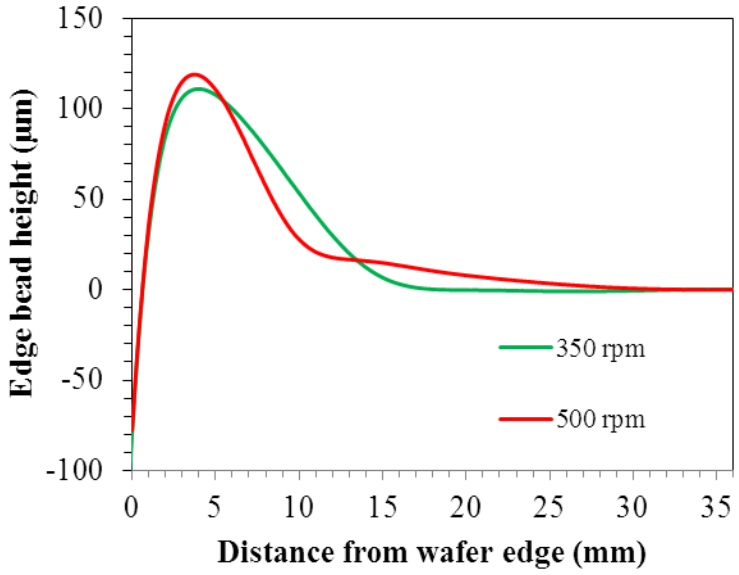

Supplementary Figure S10. Surface profiling of spin-coated PDMS layers on 3-inch silicon wafers. The PDMS is heated to 100°C directly after spin coating.

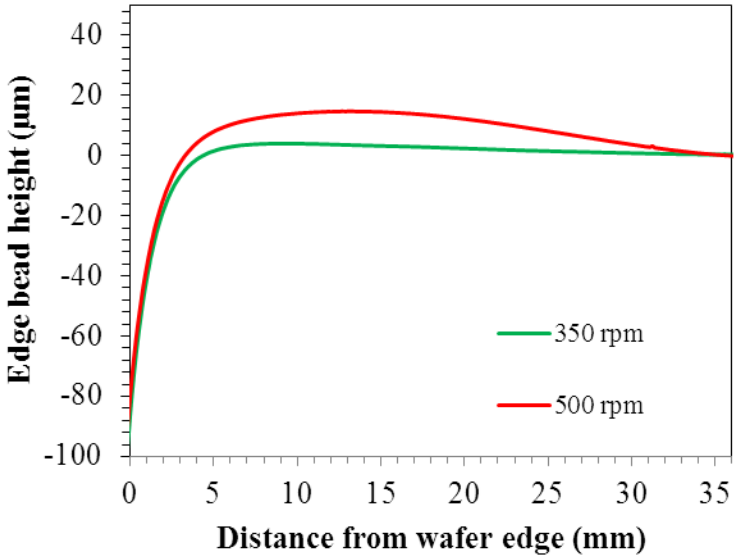

Supplementary Figure S11. Surface profiling of spin-coated PDMS layers on 3-inch silicon wafers planarized for 24 h at 20°C.

Supplementary Figures S10 and S11 show the experimental results of the surface profiling of the spin-coated PDMS samples.

7. Data generated from the study presented in tabular format

Material	Spin speed (rpm)	Edge bead height (µm)	Edge bead position (mm)	Thickness (µm)
PDMS	500	119	3.9	181
PDMS	350	111	4.5	253.8
SU-8	1000	59	4.7	119
SU-8	700	27.6	7.1	197
SU-8	400	0	-	480

Supplementary Table 3. Samples heated directly after spin coating. Hotplate temperature equals 95°C for SU-8 and 100°C for PDMS.

Material	Spin speed (rpm)	Edge bead height (µm)	Edge bead position (mm)	Thickness (µm)
PDMS	500	15	14.9	259.6
PDMS	350	3.3	10.6	372.6
SU-8	1000	57.3	3.6	140
SU-8	700	88.6	5.3	218
SU-8	400	10.6	7.4	480

Supplementary Table 4. Samples planarized for 24 h at 20°C.

Material	Spin speed (rpm)	Initial edge bead height $\boldsymbol{\delta_0}$ (µm)
PDMS	500	143(27.1)
PDMS	350	187(46.8)
SU-8	1000	63.4(22.9)
SU-8	700	138.2(65.2)
SU-8	400	90.3(78)

Supplementary Table 5. Initial edge bead height measured directly after the spin coating using the method described in the text. The standard deviations are given in brackets. They are given here as they are the principle source of error in the determination of the normalized edge height (δ/δ_0) at 24 h.

Material	Spin speed (rpm)	$\boldsymbol{\delta/\delta_0}$ (Planarized 24 h)	Average thickness (µm)	$\boldsymbol{\delta/\delta_0}$ (directly annealed)
PDMS	500	0.105	220.3	0.832
PDMS	350	0.018	313.2	0.594
SU-8	1000	0.904	129.5	0.931
SU-8	700	0.641	207.5	0.2
SU-8	400	0.1173	390.1	0

Supplementary Table 6. Numerical values for the normalized edge bead height (δ/δ_0) and the average film thicknesses calculated from the experimental data.

Supplementary References

[1] Mitra S K and Chakraborty S 2012 *Microfluidics and nanofluidics handbook: fabrication, implementation, and applications* (Roca Raton, FL: CRC Press)

[2] Zhang J, Zhou W X, Chan-Park M B and Conner S R 2005 Argon Plasma Modification of SU-8 for Very High Aspect Ratio and Dense Copper Electroforming *J. Electrochem. Soc.* **152** C716–21

[3] Shu W, Yu X, Hu R, Chen Q, Ma Y and Luo X 2017 Effect of the substrate temperature on the phosphor sedimentation of phosphor-converted LEDs *2017 18th International Conference on Electronic Packaging Technology (ICEPT)* 2017 18th International Conference on Electronic Packaging Technology (ICEPT) (Harbin, China: IEEE) pp 398–401

[4] Sötebier C, Michel A and Fresnais J 2012 Polydimethylsiloxane (PDMS) Coating onto Magnetic Nanoparticles Induced by Attractive Electrostatic Interaction *Appl. Sci.* **2** 485–95

[5] Barlow A J, Harrison G and Lamb J 1964 Viscoelastic relaxation of polydimethylsiloxane liquids *Proc. R. Soc. Lond. Ser. Math. Phys. Sci.* **282** 228–51

[6] Williams M L, Landel R F and Ferry J D 1955 The Temperature Dependence of Relaxation Mechanisms in Amorphous Polymers and Other Glass-forming Liquids *J. Am. Chem. Soc.* **77** 3701–7

[7] Fox H W and Zisman W A 1950 The spreading of liquids on low energy surfaces. I. polytetrafluoroethylene *J. Colloid Sci.* **5** 514–31

[8] Bates O K 1949 Thermal Conductivity of Liquid Silicones *Ind. Eng. Chem.* **41** 1966–8

[9] Mark J E 2009 *Polymer data handbook* (Oxford ; New York: Oxford University Press)

[10] Rolland J P, Van Dam R M, Schorzman D A, Quake S R and DeSimone J M 2004 Solvent-Resistant Photocurable “Liquid Teflon” for Microfluidic Device Fabrication *J. Am. Chem. Soc.* **126** 2322–3

[11] Schneider F, Draheim J, Kamberger R and Wallrabe U 2009 Process and material properties of polydimethylsiloxane (PDMS) for Optical MEMS *Sens. Actuators Phys.* **151** 95–9